Journal of Solid State Chemistry **154,** 398–404 (2000)
doi:10.1006/jssc.2000.8801, available online at http://www.idealibrary.com on IDEAL®

Structural and Magnetic Properties of Low D Content YMn_2 Deuteride

M. Latroche,*,[1] V. Paul-Boncour,* A. Percheron-Guégan,* F. Bourée-Vigneron,† and G. André†

*Institut Fédératif Seine Amont, Laboratoire de Chimie Métallurgique des Terres Rares, CNRS, 2 rue H. Dunant, F-94320 Thiais, France; and †Laboratoire Léon Brilloin, CE-Saclay, F-91191 Gif-sur-Yvette, France

Received April 7, 2000; in revised form May 30, 2000; accepted June 16, 2000; published online August 30, 2000

The structural and magnetic properties of $YMn_2D_{1.15}$ have been investigated by temperature-dependent neutron diffraction. Magnetic and deuterium orders appear below $T_c = 217$ K. To separate both effects and to study only magnetic ordering, hydrogen atom contribution was cancelled by preparing the compound $YMn_2(H_{0.64}D_{0.36})_{1.15}$. A noncollinear magnetic structure with 3.1 μ_B/Mn is observed. Finally the low-temperature structure was fully solved taking into account both deuterium and magnetic contributions. Whereas the deuterium atoms are randomly distributed over all the 96g sites ($Fd\bar{3}m$) above 217 K, only 12i sites in space group $P\bar{4}3m$ are occupied at low temperature.

Key Words: **diffraction; magnetic ordering; Hydride; Laves phase.**

I. INTRODUCTION

YMn_2 C15-type Laves phase compound exhibits quite complex magnetic structure and has been investigated by several groups. It was first considered as a Pauli paramagnet (1), but neutron diffraction studies (2) indicated that below 100 K there is a first-order transition to an antiferromagnetic state with 2.7 μ_B on each manganese site. A large and spontaneous increase of the volume ($\Delta V/V = 5\%$) and an anomaly of the magnetic susceptibility are observed around 100 K, accompanied by a large thermal hysteresis of 30 K. This behavior has been explained by the collapse of the manganese moments above the transition temperature. Above this transition YMn_2 behaves like a weak itinerant electron magnet (3). Further neutron diffraction studies (4) revealed an helimagnetic structure with a long period (400 Å), which was interpreted as the result of magnetic frustration between Mn spins. Next from high-resolution neutron powder diffraction (5) a tetragonal distortion ($c/a = 0.995$) was observed for YMn_2 at low temperature. In addition an antiferromagnetic propagation vector (0.018,0.003,1) corresponding to a period of 430 Å along the a axis and 2500 Å along the b axis was found.

[1] To whom correspondence should be addressed.

In such an unstable magnetic structure, modification of the cell parameter either by applying pressure (6) or by substituting Y or Mn sites with another element (7) easily changes the magnetic properties. Another way to induce magnetic structural changes in metallic compounds is hydrogen absorption. For this purpose YMn_2 hydrides are very good candidates since it is possible to prepare single-phase cubic hydrides at room temperature with good crystallinity up to 3.5 H/mol (8), leading to a continuous increase of the cell parameter up to 5.8%. For larger H content a rhombohedral distortion is observed. Single-phase rhombohedral hydrides are obtained after crossing a two-phase domain ($3.5 < x < 4.1$).

Structural and magnetic properties of the YMn_2–H_2 system have been investigated as a function of temperature for $0.1 \leq x \leq 4.3$ (9). In the paramagnetic range, all hydrides are cubic with a random distribution of hydrogen within the 96g sites ($Fd\bar{3}m$) (10). Below the magnetic ordering temperature, three different domains are observed. For the concentration range below $x \leq 1.2$ H/mol, it has been shown (11) that for $0.5 < x < 0.8$, the paramagnetic phase of the hydrides transforms at 245 K from cubic to a tetragonally distorted ($c/a < 1$) and magnetically ordered phase. Below 100 K a second transition occurs into a tetragonally distorted phase but with $c/a > 1$. In the border regions ($x < 0.5$ and $0.8 < x < 1.15$), complex behaviors with two phase ranges are observed. For $x < 0.35$ a spinodal decomposition occurs in the temperature range 100–130 K. For $x = 1$ to 3, YMn_2H_x shows a ferromagnetic behavior with an increase of T_c from 200 to 320 K and of the magnetic moment from ≈ 0.1 to 0.3 μ_B per Mn atom. For $x > 4.1$ H/mol, the magnetization strongly decreases, and recent studies indicated that rhombohedral $YMn_2H_{4.3}$ is anti-ferromagnetic below 378 K (12,13).

In a previous study (14), we undertook a temperature-dependent neutron powder diffraction study on the YMn_2D compound. A weak ferrimagnetic component and a lattice parameter jump are observed around 200 K. Below T_c both magnetic and deuterium orderings occur and the compound remains cubic down to 1.4 K. A comparison with YMn_2 shows that the thermal expansion in the paramagnetic state

0022-4596/00 $35.00

and the cell parameter increase at T_c are strongly reduced (20 times smaller). Such a result was interpreted by the decrease of spin fluctuation amplitude due to the insertion of hydrogen in the lattice. Below T_c, the diffraction pattern shows extra lines corresponding to a P mode in addition to the F one. However, since these lines were still intense at high angle, they could not be attributed only to magnetic effect and were therefore related to coexistence between magnetic and deuterium ordering. The temperature dependence of the YMn_2D compound was found to be rather complex but our recent study (11) on the phase diagram of YMn_2–H_2 in the range $0 \leq x \leq 1.2$ D/mol has shown that single-phase cubic deuterides are more likely obtained for $x \geq 1.15$ D/mol.

Below the magnetic transition temperature, it is important to separate magnetic contribution from deuterium ordering. For this purpose neutron diffraction is a well-appropriate tool, which can be used either for the localization of deuterium in deuterides or for the determination of magnetic structure. However, the two contributions cannot be easily distinguished when they occur nearly at the same temperature. Isotopic substitution (H/D) in a suitable ratio (H64%,D36%) allows one to cancel the deuterium sublattice contribution and to observe exclusively the effect of magnetic ordering. This method was successfully used in the past to study the magnetic behavior of the compound $YMn_2D_{4.3}$ (12). In this paper we report on two samples $YMn_2(H_{0.64}D_{0.36})_{1.15}$ and $YMn_2D_{1.15}$ that have been investigated by ND. The evolution of the neutron diffraction patterns of $YMn_2D_{1.15}$ from 1.4 to 300 K and the determination of the nuclear and magnetic structure at 10 K are presented.

II. EXPERIMENTAL DETAILS

An intermetallic YMn_2 sample has been prepared by induction melting of the pure components (yttrium 99.9%; manganese, 99.99%) in a water-cooled copper crucible under vacuum then under argon atmosphere to avoid sublimation of manganese. To improve homogeneity, the intermetallic was melted and turned over five times and annealed two weeks at 800°C. Homogeneity was checked by metallographic examination, which did not reveal any inclusion. The composition was checked by electron microprobe analysis leading to $Y_{0.99(1)}Mn_2$-measured stoichiometry. From powder X-ray pattern, cubic $MgCu_2$-type structure was observed with cell parameter $a = 7.681(1)$ Å.

Two batches of about 8 g of alloy were ground mechanically under argon atmosphere and were powdered to a grain size of less than 36 μm. The samples were then exposed to hydrogen and/or deuterium gas at 25°C in a volumetric device to obtain $YMn_2(H_{0.64}D_{0.36})_{1.15}$ and $YMn_2D_{1.15}$. A 200°C thermal treatment for 16 h followed by slow cooling down to room temperature was performed in order to obtain single phase homogeneous deuterides as previously reported in (8).

The neutron diffraction measurements were carried out at the Laboratoire Léon Brillouin in CE-Saclay. Diffraction pattern recorded at 10 K was obtained on the 3T2 diffractometer. The neutron wavelength was 1.225 Å, and the diffraction patterns were recorded over the angular range $6° < 2\theta < 122°$ by steps of 0.05°. The temperature-dependant diffraction patterns were recorded on the G41 diffractometer between 1.4 and 234 K in the range $15 < 2\theta < 95°$ by step of 0.1°. The wavelength was 2.427 Å. The diffraction patterns have been analyzed using Rietveld's method (15). The fitting procedure was applied using the FULLPROF program (16).

Magnetic measurements have been performed with a Manics Differential Sample Magnetometer. The sample was contained in a quartz sample holder under helium atmosphere. The temperature range extends from room temperature down to 1.5 K.

III. RESULTS

From X-ray data at 298 K, the cell parameters of $YMn_2(H_{0.64}D_{0.36})_{1.15}$ and $YMn_2D_{1.15}$ are found equal to 7.886(1) Å, which is in very good agreement with a previous study relating the cell parameter dependence to the D content (10). The ND pattern evolution of $YMn_2(H_{0.64}D_{0.36})_{1.15}$ is shown as a function of temperature in Fig. 1. Above $T = 217$ K, the patterns are refined in the C15 cubic structure ($Fd\bar{3}m$) but without any H(D) contribution, which confirms the zero neutron scattering from the H(D) mixture. However the H(D) atoms are expected to be randomly distributed within the tetrahedral sites Y_2Mn_2. At 217 K extra lines appear involving a symmetry lowering into a P mode. They are attributed to the magnetism onset, since the deuterium-ordering contribution is canceled by the H/D ratio. This is confirmed by the magnetic measure-

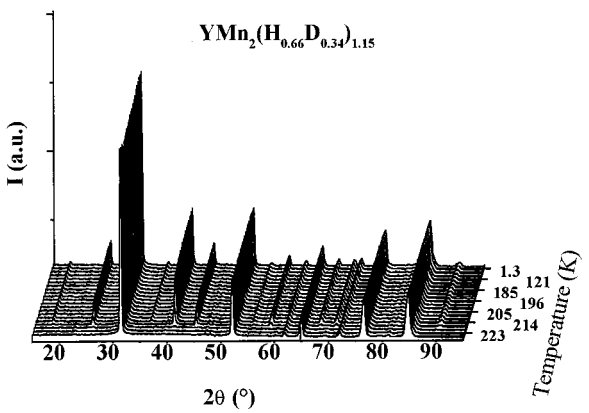

FIG. 1. Three-dimensional temperature-dependent ND pattern evolution of $YMn_2(H_{0.64}D_{0.36})_{1.15}$.

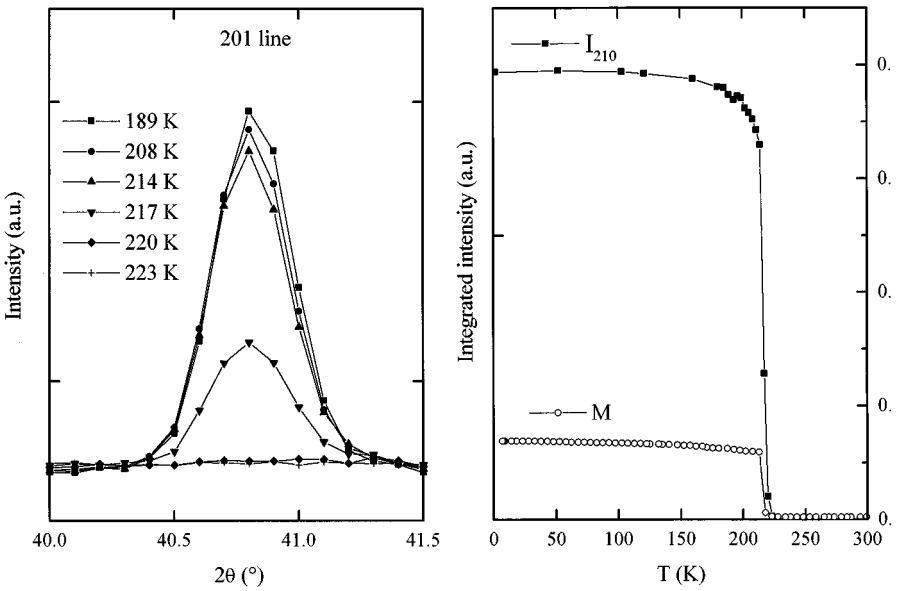

FIG. 2. Temperature evolution of a P line (201) (left) and comparison between integrated intensity $I_{(201)}$ and magnetization (right) for $YMn_2(H_{0.64}D_{0.36})_{1.15}$.

ments, which show the onset of magnetism at the same temperature (Fig. 2) and by the lattice parameter jump observed at the same temperature (Fig. 3). In Fig. 2, the typical behavior of a P line (201) is shown and compared to the magnetization that exhibits a weak ferromagnetic component (0.14 μ_B/Mn at 10 K).

According to these observations, for the low-temperature data, the equivalent positions for the compound YMn_2 have been calculated in space group $P\bar{4}3m$. The structural part was described assuming three different sites for Y and two sites for Mn (Table 1). For the magnetic part, only Mn atoms were taken into account. The Mn moments were constrained to be equal, and the weak ferromagnetic component observed in the magnetization curve but too small to be refined was neglected. Then, the low-temperature pattern ($T = 1.3$ K) could be correctly refined (Fig. 4), assuming a noncollinear anti-ferromagnetic structure (Fig. 5) with 3.10(3) μ_B/Mn.

According to the lattice constant variation as a function of the temperature and to our previous study (14) on the compound YMn_2D, it is assumed that hydrogen and magnetic ordering occur at the same temperature. The ND pattern of sample $YMn_2D_{1.15}$ recorded at 10 K exhibits P lines at the same positions as the H/D sample but with significant intensity differences. Comparison between the two patterns is shown in Fig. 6, and intensity changes are attributed to deuterium contribution.

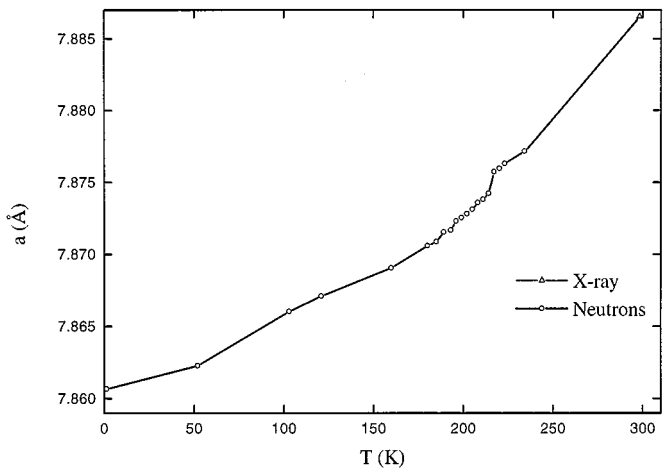

FIG. 3. Cell parameter evolution for $YMn_2(H_{0.64}D_{0.36})_{1.15}$.

TABLE 1
Equivalent Wyckoff Positions in $Fd\bar{3}m$ (Noncentro-symmetric Description) and $P\bar{4}3m$ Space Groups for $YMn_2D_{1.15}$ Deuteride

$Fd\bar{3}m$ space group			$P\bar{4}3m$ space group		
Y	8a	(0,0,0)	Y1	1a	(0,0,0)
			Y2	3c	(0,1/2,1/2)
			Y3	4e	(1/4,1/4,1/4)
Mn	16d	(5/8,5/8,5/8)	Mn1	4e	(5/8,5/8,5/8)
			Mn2	12i	(7/8,7/8,5/8)
D	96g	(7/16,7/16,1/4)	D1	12i	(7/16,7/16,1/4)
			D2	12i	(15/16,15/16,1/4)
			D3	12i	(3/16,3/16,0)
			D4	12i	(5/16,5/16,0)
			D5	24j	(3/16,11/16,1/2)
			D6	24j	(7/16,15/16,3/4)

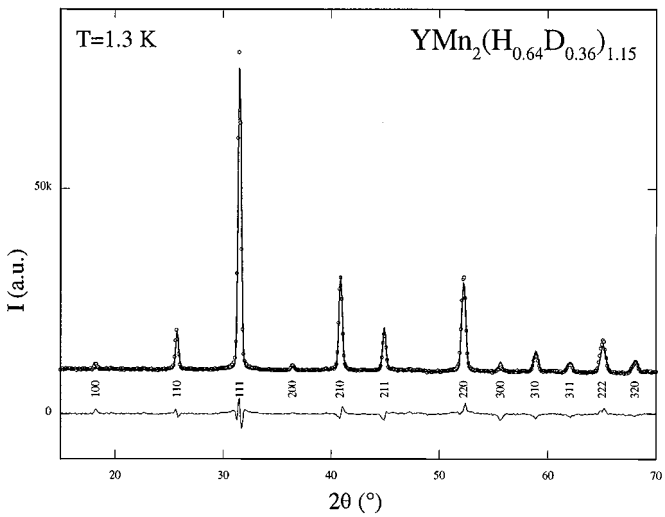

FIG. 4. Refined neutron diffraction pattern of $YMn_2(H_{0.64}D_{0.36})_{1.15}$ at 1.3 K.

In the first stage of the refinement, metal framework (Y, Mn) and magnetic structure were kept fixed to the values obtained for the (H/D) sample, and the occupancy factors of the six available tetrahedral deuterium sites Y_2Mn_2 in space group $P\bar{4}3m$ have been refined independently (Table 1). Only four sites were found significantly occupied. It is worth to note that these four sites adopt the same symmetry (12i), whereas the two other empty sites correspond to 24j ones. A rather good agreement is observed between the D content obtained from the refinement (1.26(6) D/mol) and that calculated from the solid–gas measurement (1.15(5) D/mol). Then the structure was fully refined taking into account both nuclear and magnetic contributions. It should be noted that two lines (200 and 311) are not accounted correctly. As they are correctly fitted in the H/D sample, they originate therefore from D atom ordering. It is most likely that the poor account for these two lines is due to a more complex deuterium sublattice ordering involving probably a lower symmetry. However, attempts to describe the nuclear structure in a lower symmetry ($P\bar{4}2m$ space group) did not lead to significant improvement. Moreover, it implies an increased number of parameters leading to rather unstable results. The observed, calculated, and difference patterns are shown in Fig. 7, and the results are given in Tables 2 and 3. The yttrium atoms remain in their ideal positions derived from the C15 structure but the manganese atoms are slightly shifted out (0.13(2) Å).

IV. DISCUSSION

From our data, we observed that $YMn_2D_{1.15}$ adopts a cubic symmetry with an F mode above 217 K. This is in agreement with previous works on this system for $1 < x < 3.5$ D/f.u., and it corresponds to the random distribution of the D atoms within the Y_2Mn_2 tetrahedral sites in the paramagnetic state.

Analysis of the diffraction pattern of the deuteride at $T = 10$ K shows that the four 12i sites are found significantly occupied whereas the two 24j are empty. According to Westlake (17) and Switendick (18), a deuterium site cannot be occupied if its radius is less than 0.4 Å or if the distance between two neighboring sites is less than 2.1 Å. When crossing the transition, a significant shift of the Mn atoms is observed. This involves a symmetry lowering leading to nonequivalent tetrahedral sites. In agreement with Wesltake's criterion, the 24j sites that exhibit radii equal to 0.38 and 0.35 Å respectively are found empty. However the size criterion cannot explain the different fillings of the 12i sites since the smaller site (D4) is the most occupied (Table 4). Then, the distances between D atoms (d_{D-D}) must be taken into account. For this low-content deuteride, Switendick's value of 2.1 Å is too low to be valid. However, if one admits

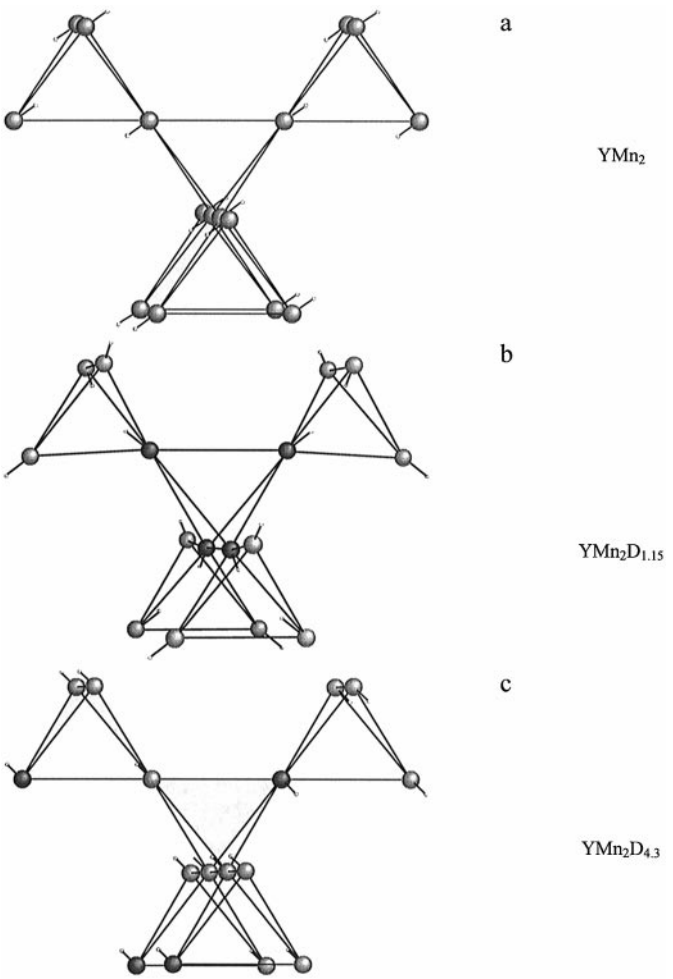

FIG. 5. (101) projection of the magnetic structure for (a) YMn_2 (4), (b) $YMn_2D_{1.15}$ (this work), and (c) $YMn_2D_{4.3}$ (12).

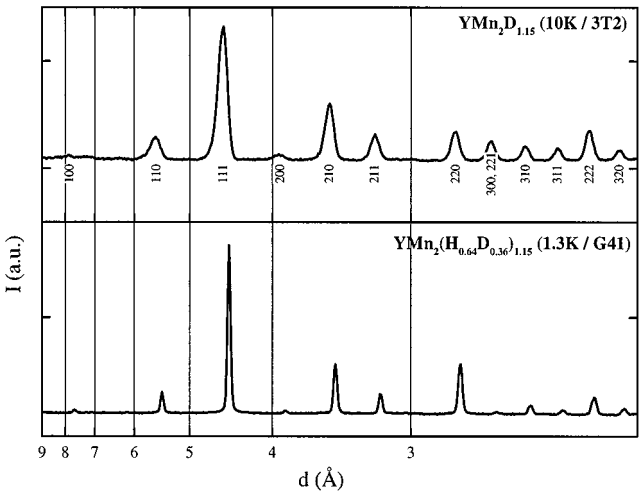

FIG. 6. Comparison between the ND patterns of $YMn_2(H_{0.64}D_{0.36})_{1.15}$ recorded on G41 at 1.3 K (bottom) and $YMn_2D_{1.15}$ recorded at 10 K on 3T2 (top). Due to the different wavelengths on both instruments, the intensities are given as a function of d spacings.

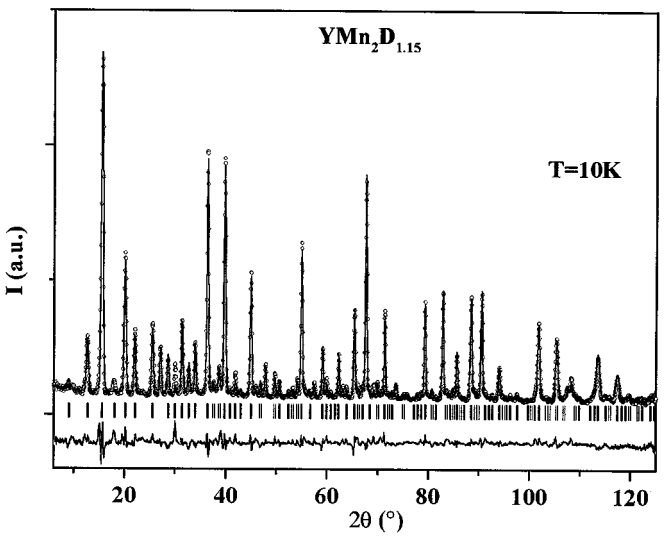

FIG. 7. Refined neutron diffraction pattern of $YMn_2D_{1.15}$ at 10 K.

that the repulsion between D atoms is still the driving force ruling the occupation of the four remaining 12i sites, a mean theoretical distance $d_{D\text{–}D}$ can be calculated according to the overall deuterium concentration. Such a calculation leads to a value of 2.86 Å. According to this value, the population of each site has been calculated and a fairly good agreement is observed with the refined one. Remarkably, the site D4 is significantly more populated than the other three because it has less neighbors at a distance less than 2.86 Å.

Concerning magnetic structure, important differences are noted if one makes comparisons with the parent compound. Whereas YMn_2 exhibits a collinear magnetic structure, the present deuteride presents a noncollinear spin arrangement. The nuclear structure involves two different Mn sites with two different symmetries (4e and 12i), and a significant shift from the ideal C15 positions is observed. It is also worth noting that according to Table 4, these Mn atoms have different environments in terms of D atoms (6 and 2 respectively). Therefore one should expect different moment beared by each atom but it was not possible to obtain stable refinement in that case.

At $T = 217$ K, a symmetry lowering to a P mode occurs with a cell parameter jump and the onset of magnetism. The crossing of the transition involves a symmetry lowering and appearance of superstructure lines. Below T_c, both deuterium and magnetic orders occur. The origin of the driving force for the transition was previously discussed for the enriched hydrogen compounds $YMn_2D_{4.3\sim5}$ (12,13) but it remains unclear which effect (H or magnetic ordering) involves the other. Pressure-dependent neutron diffraction study might be helpful in order to get a better understanding of the coupling between both effects and will be investigated in the near future.

TABLE 2
Structural Parameters for $YMn_2D_{1.15}$ Obtained at 10 K

Atoms		x	y	z	B (Å^2)	N	M (μ_B)
Y1	1a	0	0	0	0.45(2)	1	
Y2	3c	0	$\frac{1}{2}$	$\frac{1}{2}$		1	
Y3	4e	0.2504(4)	x	x		1	
Mn1	4e	0.6341(6)	x	x	0.17(3)	1	3.10(3)
Mn2	12i	0.8642(4)	x	0.6163(5)		1	
D1	12i	0.4575(19)	x	0.2685(24)	1.20(9)	0.164(16)	
D2	12i	0.9656(15)	x	0.2571(23)		0.184(8)	
D3	12i	0.1808(35)	x	0.9961(49)		0.076(8)	
D4	12i	0.3064(7)	x	0.9742(9)		0.416(12)	
	$R_{\omega p} = 8.12$	$R_{Bragg} = 7.60$	$R_{Mag} = 11.1$	Cell par.(Å) $a = 7.855(1)$		1.26(6) D/f.u.	

TABLE 3
Magnetic Structure for $YMn_2D_{1.5}$ Obtained at 10 K

Atom	x	y	z	M_x	M_y	M_z
Mn1	0.6341(6)	0.6341(6)	0.6341(6)	1.48(3)	1.93(2)	1.93(2)
4e	0.3659(6)	0.3659(6)	0.6341(6)	−1.48(3)	−1.93(2)	1.93(2)
	0.3659(6)	0.6341(6)	0.3659(6)	−1.48(3)	1.93(2)	−1.93(2)
	0.6341(6)	0.3659(6)	0.3659(6)	1.48(3)	−1.93(2)	−1.93(2)
Mn2	0.1358(4)	0.1358(4)	0.6163(5)	−1.48(3)	−1.93(2)	−1.93(2)
12i	0.1358(4)	0.6163(5)	0.1358(4)	−1.48(3)	−1.93(2)	−1.93(2)
	0.6163(5)	0.1358(4)	0.1358(4)	1.48(3)	1.93(2)	1.93(2)
	0.8642(4)	0.8642(4)	0.6163(5)	1.48(3)	1.93(2)	−1.93(2)
	0.8642(4)	0.3837(5)	0.1358(4)	1.48(3)	1.93(2)	−1.93(2)
	0.3837(5)	0.8642(4)	0.1358(4)	−1.48(3)	−1.93(2)	1.93(2)
	0.8642(4)	0.1358(4)	0.3837(5)	1.48(3)	−1.93(2)	1.93(2)
	0.8642(4)	0.6163(5)	0.8642(4)	1.48(3)	−1.93(2)	1.93(2)
	0.3837(5)	0.1358(4)	0.8642(4)	−1.48(3)	1.93(2)	−1.93(2)
	0.1358(4)	0.8642(4)	0.3837(5)	−1.48(3)	1.93(2)	1.93(2)
	0.1358(4)	0.3837(5)	0.8642(4)	−1.48(3)	1.93(2)	1.93(2)
	0.6163(5)	0.8642(4)	0.8642(4)	1.48(3)	−1.93(2)	−1.93(2)

Note. $M = 3.10(3)\ \mu_{B/Mn}$.

Due to the cell volume increase related to hydrogen absorption, the transition crossing does not involve a significant volume jump as is observed for YMn_2. It shows that the Mn moments are already localized in the paramagnetic state. If one compares the magnetic structure of $YMn_2D_{1.15}$ to that of the YMn_2 parent compound, it is worth noting that the incommensurate helimagnetic propagation vector is not observed. In addition, the F mode no longer exists. For larger hydrogen content up to $x = 4.5$, a commensurate collinear antiferromagnetic structure is found. Those differences are seen in Fig. 5. It shows the great sensitivity of the YMn_2–H_2 system to the hydrogen content.

This is obviously connected to the H concentration, and for a better understanding of the magnetic properties, the effect of filling the 3d band with electrons coming from the hydrogen should be considered. Band structure calculations (19) have shown that for YMn_2 hydrides, an additional ferrimagnetic component must appear. Unfortunately, such calculations do not make it possible to explain the collinear or noncollinear behavior of the magnetic structure. It will therefore be interesting to perform the neutron diffraction study of intermediate concentrations (which are currently in progress for $x = 2$ and 3) in order to follow the evolution of the magnetic structure as a function of hydrogen content.

TABLE 4
Manganese and Deuterium Atom Environments for $YMn_2D_{1.15}$ at 10 K

D atoms		Environment (Å)		Site radius (Å)	% occupancies observed	% occupancies calculated for $d_{D-D} > 2.86$ Å
Mn1	4e	6 D1	1.74(3)			
		3 Mn1	2.99(1)			
		3 Mn2	2.55(1)			
Mn2	12i	2 D4	1.71(2)			
		1 Mn1	2.55(1)			
		2 Mn2	2.75(1)			
		2 Mn2	2.81(1)			
		1 Mn2	3.02(1)			
D1	12i	1 Y2	2.16(2)	0.41	16.4	19
		1 Y3	2.30(3)			
		2 Mn1	1.74(3)			
D2	12i	1 Y1	2.05(2)	0.43	18.4	14
		1 Y3	2.40(2)			
		2 Mn2	1.85(3)			
D3	12i	1 Y1	2.01(4)	0.43	7.6	11
		1 Y3	2.14(5)			
		2 Mn2	1.93(5)			
D4	12i	1 Y2	2.16(1)	0.40	41.6	37
		1 Y3	2.26(1)			
		2 Mn2	1.71(2)			

V. CONCLUSION

To conclude, $YMn_2D_{1.15}$ adopts a cubic structure above T_c with randomly distributed D atoms within the 96g tetrahedral sites. Below T_c, both deuterium and magnetic orders occur with a symmetry lowering. Taking advantage of the zero contribution of the H/D mixture in ND, magnetic order has been independently determined and the full structure determination has been achieved at 10 K for the deuterated compound.

REFERENCES

1. K. H. J. Buschow and R.C. Sherwood, *J. Appl. Phys.* **48,** 4643 (1977).
2. Y. Nakamura, M. Shiga, and S. Kawanowo, *Physica B* **120,** 212 (1983).
3. T. Freltoft, P. Böni, G. Shirane, and K. Motoya, *Phys. Rev. B* **37,** 3454 (1988).
4. A. Ballou, J. Desportes, R. Lemaire, Y. Nakamura, and B. Ouladdiaf, *J. Magn. Magn. Mat.* **70,** 129 (1987).
5. R. Cywinski, S.H. Kilcoyne, and C. A. Scott, *J. Phys.: Condens. Matter* **3,** 6473 (1991).
6. R. Hauser, E. Bauer, E. Gratz, Th. Häufler, G. Hilscher, and G. Wiesinger, *Phys. Rev. B* **50,** 13493 (1994).
7. M. Shiga, H. Wada, H. Nakamura, K. Yoshimura, and Y. Nakamura, *J. Phys. F* **17,** 1781 (1987).
8. J. Przewoznik, V. Paul-Boncour, M. Latroche, and A. Percheron-Guégan, *J. Alloys Compd.* **232,** 107 (1996).
9. H. Fujii, M. Saga, and T. Okamoto, *J. Less Common Met.* **130,** 25 (1987).
10. M. Latroche, J. Przewoznik, V. Paul-Boncour, A. Percheron-Guégan, and F. Bourée-Vigneron, *J. Alloys Compd.* **231,** 99 (1995).
11. H. Figiel, J. Przewoznik, V. Paul-Boncour, A. Lindbaum, E. Gratz, M. Latroche, M. Escorne, A. Percheron-Guégan, and N. P. Mietnowski. *J. Alloys Compd.* **274,** 29 (1998).

12. I. N. Goncharenko, I. Mirebeau, A. V. Irodova, and E. Suard, *Phys. Rev. B* **56,** 2580 (1997).
13. M. Latroche, V. Paul-Boncour, A. Percheron-Guégan, and F. Bourée-Vigneron. *J. Alloys Compd*. **274,** 59 (1998).
14. M. Latroche, V. Paul-Boncour, A. Percheron-Guégan, F. Bourée-Vigneron, and G. André, *Physica B* **234–236,** 599 (1997).
15. H. M. Rietveld, *Acta Crystallogr.* **22,** 151 (1967).
16. J. Rodríguez-Carvajal, *in* "Abstracts of Satellite Meeting on Powder Diffraction, Congr. Int. Union of Crystallography, Toulouse, France," p. 127, (1990).
17. D. G. Westlake, *J. Less-Common Met*. **90,** 251 (1983).
18. A. C. Switendick, *Z. Phys. Chem*. **117,** 89 (1979).
19. M. Pajda, R. Ahuja, B. Johansson, J. M. Wills, H. Figiel, A. Paja, and O. Eriksson, *J. Phys.: Condens. Matter* **8,** 3373 (1996).